

LA-UR-04- 0 777

Approved for public release;  
distribution is unlimited.

*Title:* A STUDY OF TWO-BODY FORCES IN FLUIDIZATION

*Author(s):* Bryan A. Kashiwa and Rick M. Rauenzahn  
Theoretical Division, Fluid Dynamics Group

*Submitted to:* Paper submitted for publication in proceedings of  
3rd International Conference on Two-Phase Flow Modelling  
& Experimentation, Pisa, ITALY  
22-24 SEP 2004



Los Alamos National Laboratory, an affirmative action/equal opportunity employer, is operated by the University of California for the U.S. Department of Energy under contract W-7405-ENG-36. By acceptance of this article, the publisher recognizes that the U.S. Government retains a nonexclusive, royalty-free license to publish or reproduce the published form of this contribution, or to allow others to do so, for U.S. Government purposes. Los Alamos National Laboratory requests that the publisher identify this article as work performed under the auspices of the U.S. Department of Energy. Los Alamos National Laboratory strongly supports academic freedom and a researcher's right to publish; as an institution, however, the Laboratory does not endorse the viewpoint of a publication or guarantee its technical correctness.

Form 836 (8/00)



# A STUDY OF TWO-BODY FORCES IN FLUIDIZATION

(LA-UR-04-\_\_\_\_)

*Bryan A. Kashiwa and Rick M. Rauenzahn  
Theoretical Division, Fluid Dynamics Group  
Los Alamos National Laboratory*

Paper submitted for publication in proceedings of  
3<sup>rd</sup> International Conference on Two-Phase Flow Modelling & Experimentation,  
Pisa, ITALY  
22-24 SEP 2004

## ABSTRACT

The effect of two-body forces on the structure of dynamic waves in fluidized beds is studied, with particular emphasis on expansion waves. Averaged equations of motion are used for the study, so the media appear to be interpenetrating continua. Both inertial and viscous two-body effects are considered for incompressible materials fluidized by an incompressible fluid. Inertial effects are included in the averaged momentum exchange force, using exact (classical) results for the potential flow generated by the motion of one submerged body relative to another body. Viscous effects are represented, in the limit of zero relative Reynolds number, by solutions to Stokes' equations for the two-body problem. For simple one-dimensional motion the inertial force is repulsive always, giving a positive compressibility to the dispersed field total density; the force is of such a magnitude that the single-pressure continuum equations are unconditionally hyperbolic. The corresponding 1-D viscous force is attractive when the bodies move apart, and therefore introduces a negative compressibility to the dispersed field. Competition between the two-body inertial and viscous forces ultimately determines the nature of dynamic waves in a given fluidization system.}

*This work was carried out under the auspices of the National Nuclear Security Administration of the U.S. Department of Energy at Los Alamos National Laboratory under Contract No. W-7405-ENG-36.*

# A STUDY OF TWO-BODY FORCES IN FLUIDIZATION

Bryan A. Kashiwa (bak@lanl.gov) and Rick M. Rauenzahn (rick@lanl.gov)

Los Alamos National Laboratory†

Los Alamos, NM 87544 USA

## ABSTRACT

The effect of two-body forces on the structure of dynamic waves in fluidized beds is studied, with particular emphasis on expansion waves. Averaged equations of motion are used for the study, so the media appear to be interpenetrating continua. Both inertial and viscous two-body effects are considered for incompressible materials fluidized by an incompressible fluid. Inertial effects are included in the averaged momentum exchange force, using exact (classical) results for the potential flow generated by the motion of one submerged body relative to another body. Viscous effects are represented, in the limit of zero relative Reynolds number, by solutions to Stokes' equations for the two-body problem. For simple one-dimensional motion the inertial force is repulsive always, giving the a positive compressibility to the dispersed field total density; the force is of such a magnitude that the single-pressure continuum equations are unconditionally hyperbolic. The corresponding 1-D viscous force is attractive when the bodies move apart, and therefore introduces a negative compressibility to the dispersed field. Competition between the two-body inertial and viscous forces ultimately determines the nature of dynamic waves in a given fluidization system.

## 1. INTRODUCTION

Among the great many outstanding problems in the science called "two-phase flow" is the determination of the speed and structure of dynamic waves in fluidized beds [1]. Two-phase dynamic waves, in the one-dimensional approximation of a fluidized bed, form the subject of this paper. Of interest is the manner in which 1-D multibody forces may affect the nature of these well-known dynamic waves. (As will be made clear below, we prefer the more general term "multifield" to describe this science.)

A simple fluidized bed is created by the upward flow of fluid (gas or liquid) in a vertical tube containing a packed bed of solid grains, initially resting on a grid at the tube bottom. A pump furnishes the power needed to make the fluid flow upward through the grid, through the bed of grains, and through the tube. As the fluid speed is slowly increased a point is reached at which the grains become levitated by the fluid, so the weight of the grain bed is no longer born by the grid. The flow at this point is said to be at the minimum fluidization velocity  $U_{mf}$ . As the flow speed is increased further, and then held fixed, the bed expands so that the free surface reaches a constant height in the tube. Although the grains may be moving in some general pattern in the tube between the grid and the free surface of the bed, the velocity of the grains, averaged on the entire tube, is zero. For this reason the bed is called a fixed fluidized bed (rather than a traveling bed or fast fluidized bed). The fraction of the tube volume occupied by the grain material can be observed by measuring the height of the free surface. For all flow speeds  $U$  that are lower than the terminal velocity of one grain  $U_T$ , there will be a single (averaged) volume fraction of the solid grains in the bed  $\theta(U)$ .

Now consider a small increase in  $U$ , accomplished very quickly by a sudden change in pump speed. The bed will begin to rise uniformly, at a rate determined by the force acting between the fluid

and the grains. Because no additional grains enter the tube at the grid, a lower value of  $\theta$  will immediately arise at the grid and propagate upward toward the free surface. Conversely a small sudden decrease in  $U$  will be accompanied by a uniform downward motion of the bed. Because no grains leave the tube at the grid, a larger value of  $\theta$  will occur there and propagate upward toward the free surface. Hence any change in  $U$  such that the fluidization speed is between  $U_{mf}$  and  $U_T$  will result in adjustment in the bed  $\theta$  that is accomplished over time by an upward moving wave, originating at the grid. In general the speed and structure of the rising wave depends on the dynamics of the interacting materials. Hence these are dynamic waves rather than continuity (kinematic) waves.

In the science of gas dynamics the study of dynamic waves is accomplished in the frame of reference of the moving wave, which is typically not the frame of a moving element of mass. In the wave frame, the positive direction is the direction of the wave (relative to a laboratory observer); let us call the uniform state in the positive direction the "right" side of the wave, and let the other side be the "left". The decrease in  $U$  causes an increase in total mass density on the left; in the lexicon of gas dynamics this is called a compression wave. The increase in  $U$  causes a decrease in mass density on the left, so this would be called an expansion wave (or rarefaction). The wave structure is the variation of the velocities and densities between the left and right uniform states; the left state being the new density, and the right corresponding to the density prior to the step change in  $U$ . The "width" of the 1-D wave is the distance spanned between the left and right uniform states.

Of course any physical fluidized bed exhibits multidimensional motions. That is, across any horizontal plane in the tube, the state can be quite different from point to point. This is because the grid at the bottom cannot assure a perfectly uniform inflow, and because of the inherent (Rayleigh-Taylor) instability associated with the

---

†By acceptance of this article, the publisher recognizes that the U.S. Government retains a nonexclusive, royalty-free license to publish or reproduce the published form of this contribution, or to allow others to do so, for U.S. Government purposes. This is work performed under the auspices of the U.S. Department of Energy.

levitation of a heavy material (the grains) with the impulse of a lighter material (the fluid) in a gravitational field. In many applications the formation of voidage bubbles due to this instability is an undesirable feature because large volumes of the fluid will not come into contact with the grains. Such contact may be the goal of a fluidized bed chemical reactor, for example. Nevertheless, the study of multidimensional phenomena necessarily begins with a sound understanding of the 1-D behavior of the system. For this reason attention is confined here to the 1-D approximation, which is approached to a satisfactory degree in the laboratory by choosing a tube diameter that is not too large compared to the average spacing of the grains in the bed. In this way the horizontal variation in the multidimensional motions is minimized by the tube walls.

The fluidized bed in a narrow tube is a relatively simple device to construct in the laboratory, and the waves are easily observed through a clear tube wall. Unfortunately the quantitative measurement of the wave speeds and wave structures is difficult owing to the finite width of the waves, and to finite multidimensionality. An ingenious experiment that facilitates measurement of the expansion wave was developed by G. B. Wallis; a second grid is placed at the top of the tube so that for  $U > U_T$  a "stack" of grains is held at the top grid. By reducing the flow speed to somewhat below  $U_T$ , but above  $U_{mf}$  grains will fall from the stack, and a very clearly defined wave rises through the stack toward the upper grid. At  $U < U_{mf}$  the entire stack falls away from the upper grid, and a sharp wave moves into the stack as it falls.

Data from this experiment are reported by Wallis *et al.* [1], who referred to the expansion wave as a "decompression" wave, and made important progress relative to forming a physical mechanism explaining the data. Unfortunately a full mechanistic explanation of the data is still lacking.

The main purpose of the present work is to study the possibility that certain two-phase flow wave phenomena are controlled by the momentum transfer between the interacting materials – *as affected by the forces between neighboring bodies transmitted by the intervening fluid*. To begin, the force contribution due to two interacting bodies is considered, with both inertial and viscous contributions included. The goal is to find the lowest-order model that contains these effects, and to observe the nature of the model in terms of physical expectations. [Remark: Studies of this sort are not unique. For this reason, remarks like this are inserted in the text to highlight where the present work deviates from, or adheres to, the norm established in the literature.]

A second, more distant, purpose of this study is to find an appropriate set of averaged equations of motion that can be used for so-called Large-Eddy-Simulations of multifield turbulence. Numerical LES has been helpful for modeling closures for single-fluid turbulence theories, and are based on the Euler equations from gas dynamics. However, there exists a serious roadblock to multifield LES: the multifield analog of the Euler (nonviscous) equations are not hyperbolic. This means that numerical calculations on a very fine grid can possess nonphysical wave structures that cannot be included in LES statistics; and separation of the physical wave data from the nonphysical data is impossible. Hence a reliable, physically-based, nonviscous multifield model would finally enable multifield LES turbulence closures.

The plan for the paper is as follows. Section 2 is a brief discussion of the origin of the averaged equations most commonly

used for multifield flow in the limit of incompressible materials. Section 3 shows the origin of what is called the "standard" force for the interaction among material fields, on average. Section 4 is the development of the two-body potential flow (inertial) force density; and Sec. 5 develops the corresponding two-body viscous force. Section 6 displays the character of the 1-D equations, and Sec. 7 is a summary.

## 2. AVERAGED EQUATIONS

A wide variety of methods have been used to obtain averaged equations for multiple interacting materials. One of the most widely accepted approaches uses ensemble averaging of an exact (closed) set of dynamical equations [2,3,4]. The ensemble average makes continuous variables out of discontinuous ones; so the result is a set of continuum equations. The continuum equations for multiple fields are needed in this study. In order to make it clear where it is that the two-body forces fit into this framework, a brief description of the averaging process is given here.

Consider  $N$  different materials, only one of which can reside at a location in space-time  $(\mathbf{x}, t)$ . Let the state at a space-time point be described by the material density, velocity, stress, and  $\mathcal{H}$  function:  $[\rho_o, \mathbf{u}_o, \boldsymbol{\sigma}_o, \alpha_r]$ . The subscript  $o$  signifies a point in space-time, and the integer subscript  $r$  is a material number such that  $1 \leq r \leq N$ . The state evolves according to conservation of mass, momentum, volume, and material type. With no change in material type (no phase change) the exact equations for this evolution are

$$\dot{\rho}_o + \rho_o \nabla \cdot \mathbf{u}_o = 0 \quad (1a)$$

$$\rho_o \dot{\mathbf{u}}_o - \nabla \cdot \boldsymbol{\sigma}_o - \rho_o \mathbf{g} = 0 \quad (1b)$$

$$\nabla \cdot \mathbf{u}_o = 0 \quad (1c)$$

$$\dot{\alpha}_r = 0 \quad (1d)$$

where the overdot signifies the Lagrangian derivative along  $\mathbf{u}_o$ . If the stress is represented by an isotropic hydrodynamic pressure plus a viscous deviator this is a closed set of equations (otherwise a stress evolution equation is needed). The parameter  $\alpha_r$  has a value of one if  $r$ -material is at the space-time point, and zero otherwise. This function has been called the "material selector" [2], "function of presence" [3], and other things by different authors. We prefer the term  $\mathcal{H}$  function, following Saffman [5], who seems to have been the originator, and who furnishes the essential rules of applying the ensemble average to quantities that are multiplied by it.

Here we let angle brackets indicate the ensemble average, which can be thought of as a sum over a great many observations of the state at a point in space-time. These averages are referred to as the "mean", and the  $r$  index refers to the material "field". The mean field variables are continuous ones generated by the  $\mathcal{H}$ -weighted ensemble average of discontinuous variables. Of particular interest are the mean mass density, mean momentum density, and mean  $r$ -field stress, defined respectively by

$$\rho_r = \langle \alpha_r \rho_o \rangle \equiv \text{mean } r\text{-field total mass density} \quad (2a)$$

$$\rho_r \mathbf{u}_r = \langle \alpha_r \rho_o \mathbf{u}_o \rangle \equiv \text{mean } r\text{-field momentum density} \quad (2b)$$

$$\boldsymbol{\sigma}_r = \langle \alpha_r \boldsymbol{\sigma}_o \rangle \equiv \text{mean } r\text{-field stress} \quad (2c)$$

whose evolution equations may be expressed in terms of the averages

$$\theta_r = \langle \alpha_r \rangle \equiv \text{mean } r\text{-field } \mathcal{H} \text{ function} \quad (2d)$$

$$\sigma = \langle \sigma_o \rangle \equiv \text{mean mixture stress} \quad (2e)$$

having associated fluctuational parts defined

$$\mathbf{u}'_r = \mathbf{u}_o - \mathbf{u}_r \equiv r\text{-field velocity fluctuation} \quad (2f)$$

$$\sigma' = \sigma_o - \sigma \equiv \text{stress fluctuation} \quad (2g)$$

with averages of the velocity fluctuation giving the all-important multiphase Reynolds stress density

$$\rho_r \mathbf{R}_r = \langle \alpha_r \rho_o \mathbf{u}'_r \mathbf{u}'_r \rangle \equiv r\text{-field Reynolds stress density.} \quad (2h)$$

Equations for the time evolution of  $\rho_r$  and  $\mathbf{u}_r$  are formally obtained by taking the time derivative of the definition itself, and rearranging with the help of the exact equations. The result is a set of expressions that look just like conservation equations for mass and linear momentum with a momentum exchange term and turbulence effect added on. The additional terms still require models, so the closure modeling still remains to be done. The unclosed equations are,

$$\dot{\rho}_r + \rho_r \nabla \cdot \mathbf{u}_r = 0 \quad (3a)$$

$$\rho_r \dot{\mathbf{u}}_r - \theta_r \nabla \cdot \sigma - \rho_r \mathbf{g} = \nabla \cdot \theta_r (\sigma_r - \sigma) - \langle \sigma' \cdot \nabla \alpha_r \rangle - \nabla \cdot \rho_r \mathbf{R}_r \quad (3b)$$

$$\nabla \cdot \mathbf{u} = 0 \quad (3c)$$

$$\theta_r - \rho_r v_r = 0 \quad (3d)$$

where  $\mathbf{u} = \sum_{s=1}^N \theta_s \mathbf{u}_s$ ,  $v_r$  is the specific volume of  $r$ -material, and the overdot with subscript  $r$  is used to signify the Lagrangian derivative relative to the mean motion of  $r$ -material. That is  $(\cdot)_r = \partial(\cdot)/\partial t + \mathbf{u}_r \cdot \nabla(\cdot)_r$ . The isotropic part of the mean stress is the hydrodynamic pressure  $\sigma = -p\mathbf{I}$ , the deviatoric part is neglected here. Equation (3c) formally comes from the evolution equation for  $p$ , in the limit of constant  $v_r = 1/\rho_r^o$ . The mean pressure evolution equation is constructed by making the assumption

$$\langle \alpha_r \rangle \equiv \theta_r = \rho_r v_r(p, T_r) \quad (4)$$

where  $T_r$  is the mean  $r$ -temperature, and where  $v_r(p, T_r)$  is the caloric equation of state for pure  $r$ -material. The equation for  $\dot{p}$  comes from the identity  $[1 - \sum_{s=1}^N \theta_s] = 0$ , which can be placed in rate form by differentiation with respect to time. In the isothermal, incompressible limit (with no phase change), Eq.(3c) is exact; its genesis is the assumption made in Eq.(3d), which is a statement of the averaged equation of state for the  $r$ -field [4].

The system Eq.(3) is the ensemble average of the system Eq.(1), using the collection of definitions given in Eq.(2). System Eq.(3) is displayed this way to emphasize that the averaged equations look just like the exact equations, but with extra (unclosed) terms on the right side of the momentum equation.

The first term on the right side of Eq.(3b) is an acceleration due to the difference between the  $r$ -stress and the mean stress  $(\sigma_r - \sigma)$ , which arises, for example, when grains in the fluidized bed come into direct contact. In this example the stress difference has been called a "configuration" stress, because it depends on the topological orientation of a packed bed of grains. The configuration stress leads to waves that depend on the elastic properties of the grains themselves. Simple models exist for the configuration stress [4] but are not needed in this paper.

The second term on the right side of Eq.(3b) is the exchange force density. The gradient of the  $\mathcal{H}$  function is a vector (with

units of inverse length) pointing into  $r$ -material [5]; it is nonzero only at an interface. Hence the ensemble average is the net force on the  $r$ -field, as a result interaction with all of the other materials (any *one* of which can be on the other side of the interface). Because the average is impossible to evaluate exactly, except for trivial cases, we express the exchange force symbolically by

$$-\langle \sigma'_r \cdot \nabla \alpha_r \rangle = \sum_{s=1}^N \mathbf{f}_{rs}. \quad (5)$$

(The sum works out alright because  $\mathbf{f}_{ss} = 0$ .) There exist many ways to approximate the force term, some of which are given in the various texts on this subject [6,7 for example], much of which is sketched in the next section. The following section is offered in order to place the present work into proper context with the commonly known ways of making this important approximation.

### 3. THE "STANDARD" FORCE

Because of the enormous variety of possible multifield flows, there can be no single expression for the force density  $\mathbf{f}_{rs}$  that applies in all cases. Hence the force density must be modeled on a case-by-case basis. Nevertheless it is possible to distill from the vast multifield literature [2,4,6,7,8,9,10 for example], an expression for  $\mathbf{f}_{rs}$  that contains most of the physical features currently in common use, with the case-specific data left as parameters. In this paper, the functional form of this force density is called the "standard force", whose origins are discussed briefly as a reminder of the assumptions that are applied in its derivation.

Consider a single arbitrary rigid body in steady motion  $w$  relative to a stationary infinite fluid of density  $\rho_f^o$ . The component of total force acting the body in the direction of motion is  $-C_d \frac{1}{2} \rho_f^o w^2 A$ , where  $C_d$  is a drag coefficient and  $A$  is the cross-sectional area of the body. This force contains the effects of flow separation (pressure) and fluid viscous stress; it is to be averaged and placed into general coordinates. The standard way to do this is to suppose that there exist a great many bodies of identical nature each of which contributes a like amount to the total force on the entire collection, which is the field of dispersed bodies. Let  $\theta_s$  be the fraction of the total volume occupied by the field of like bodies. Then  $\theta_s = nV_s$  where  $n$  is the number density of bodies, and  $V_s$  is the volume of one body. The force density acting on the field is then  $-(\frac{1}{2} A/V_s) \theta_s C_d \rho_f^o w^2$ , on average. This is typically called the drag force.

Now suppose that the fluid "field" really has an arbitrary (space-time varying), but averaged, velocity  $\mathbf{u}_f$  in the laboratory frame of reference; likewise suppose that the collection of bodies has an averaged center-of-mass velocity  $\mathbf{u}_s$ . Further suppose that there exists a gradient in averaged pressure that causes an (identical) acceleration of each body in the collection. Because the pressure gradient appears separately in the averaged equation of motion for the field, and because the drag force implicitly contains the pressure gradient, a factor of  $(1 - \theta_s) = \theta_f$  is applied to the foregoing force density. Hence in general coordinates the drag force density on the  $s$ -field, is  $-(\frac{1}{2} A/V) \theta_s \theta_f C_d \rho_f^o |\mathbf{u}_s - \mathbf{u}_f| (\mathbf{u}_s - \mathbf{u}_f)$ . The functional form of this force density, appearing frequently in the literature [4,7], is,

$$\mathbf{f}_{sf} = -\mathcal{K}_{sf} \theta_s \theta_f (\mathbf{u}_s - \mathbf{u}_f) \quad (6a)$$

where the scalar exchange coefficient is

$$\mathcal{K}_{sf} = \frac{3}{4} C_d \rho_{sf}^o |\mathbf{u}_s - \mathbf{u}_f|/d \quad (6b)$$

in which the factor  $\frac{3}{4}$  corresponds to spheres of averaged diameter  $d$ , and the appropriate material density is designated by  $\rho_{sf}^o$ , which may be either the s- or f-field material density, depending on the definition of  $C_d$  (and on which field is declared to be “continuous”). About the only known exact value of  $C_d$  is that for the very slow motion of a single sphere in an infinite viscous fluid,  $C_d = 24/Re$ , of course due to Stokes, and valid for relative Reynolds number  $Re$ , based on the fluid viscosity and  $d$ , such that  $Re < 1$ . For any other case (non-sphere,  $Re > 1$ , time-unsteady, ...) an experimental correlation is required.

It is almost universal practice to superpose (add) additional contributions to  $\mathbf{f}_{sf}$  that arise from other physical effects. (This practice is so common that it is very easy to forget that the superposition is itself an approximation. It is one that will be followed in succeeding sections.) Perhaps the best known of the superposed force contributions is that due to time-unsteady motions; it is known variously as the “added mass”, “virtual mass”, “inviscid”, or “potential flow” force. This is most commonly estimated as a purely inertial process that is a consequence of the displacement of fluid by a submerged body. As the body accelerates it must move fluid out of its way, so the force needed to create the acceleration increases with the amount of fluid displaced. Because only the inertial part of the fluid displacement is considered, the force depends only on the fluid material density and the acceleration. And because potential flow theory is used almost exclusively to determine the force, the term “potential flow force” will be used here.

For the case of a *single* submerged body (replicated many times, to form a field) in a uniform flow, the results from the literature are almost always the same: the force depends on the difference in the Lagrangian acceleration of the two interacting fields, and acts in such a way to reduce the relative acceleration. When a nonuniform flow field is permitted (that is, one with gradients in velocity) an additional force appears that is proportional to the mean relative velocity, and acts perpendicular to it – this is a potential flow “lift” force [8].

Because the literature on the potential flow forces is very accessible, the results are simply used here and placed in the form needed for this paper. Hence the standard force becomes, finally,

$$\begin{aligned} \mathbf{f}_{rs} = & -\mathcal{K}_{rs} \theta_r \theta_s (\mathbf{u}_r - \mathbf{u}_s) - C_a \rho_{rs}^o \theta_r \theta_s (\dot{\mathbf{u}}_r - \dot{\mathbf{u}}_s) \\ & - C_a \rho_{rs}^o \theta_r \theta_s (\mathbf{u}_r - \mathbf{u}_s) \cdot 2\mathbf{W}_f \quad (7) \end{aligned}$$

where the first right side term is the drag force density, derived above. The second term is the single-body potential flow force with coefficient  $C_a = \frac{1}{2}$  for uniform rigid spheres. The third term is the Drew & Lahey [8] lift force, with antisymmetric f-strain rate  $\mathbf{W}_f = \frac{1}{2} (\nabla \mathbf{u}_f - \nabla \mathbf{u}_f^T)$  where the subscript f signifies the “continuous field” index number. Of course Eq.(7) is simply a functional form, and not a specification for  $\mathbf{f}_{rs}$ ; particular values of the coefficients, furnished by the analyst, make the equation into a specification. There still exists substantial “art” in the process of selecting the coefficients, and there is widespread disagreement on the best way to do so for any well-defined multiphase flow problem. [Remark: It is common practice, but by no means

universal, to obtain vector-valued averaged forces by averaging scalar-valued forces. The practice is successful in multifield problems because there is a single dominant direction, which is that of the averaged relative velocity. The method of making vector forces out of scalar ones, along with the superposition of forces, are practices that will be retained in this paper.]

Finally, the effects of turbulence as manifested through the multiphase Reynolds stress forms another (but not necessarily separate) important and unresolved problem. Multiphase turbulence is an equally artful modeling endeavor that is not addressed here, but must be kept in mind in any discussion of multifield phenomena. (See [11] for a good discussion.)

#### 4. THE TWO-BODY POTENTIAL FLOW FORCE

Multibody inertial forces in two-phase flow have been developed in the literature. For example Zhang & Prosperetti [12] used a configuration space method to affect an ensemble average of a potential flow about rigid bodies. Fernández *et al.* [13] considered two rigid bodies submerged in an infinite fluid to obtain the two-body force arising from motions both in the line of centers and perpendicular to the line of centers in a potential flow. Their averaging technique required assuming a form of the radial probability distribution function for the presence of the second sphere, and integrating to infinite separation radius. Unfortunately results from the literature are not in a form useful for the present purposes. This is because we wish to use potential flow solutions that are expressible in analytic form (rather than that of an infinite series), and valid for very close-spacing of the submerged grains. In both the potential flow case and the viscous (Stokes) flow case, analytic solutions appear in the form of infinite series. Numerical coefficients arise in both cases that can be parameterized by the separation of the two bodies. These coefficients can be expressed by fitting to a simple functional involving the series expansion parameter itself, as was shown by Batchelor & Green [14] for the viscous flow case of two spheres. Here we accomplish the analogous task for the potential flow of two identical spheres.

For the study performed here the simple technique used is related to that of Drew & Lahey [8], and also to that of Fernández *et al.* [13]. This method begins with the total force on a certain body and performs an average on it, assuming a linear variation in the averaged velocity of the grain field. It is possible that the configuration space method, pioneered by Batchelor [15] and utilized by Zhang & Prosperetti [12], would produce more accurate results by including the spatial variation in the grain field volume fraction as well as the velocity variation. For now the interest is in finding the lowest-order physical effect, so a more transparent method is considered sufficient, at least for now.

The analysis uses classical methods from the literature summarized long ago by Lamb [16]. Briefly, an infinite, incompressible, nonviscous, fluid is considered in which two bodies are submerged. The fluid is at rest infinitely far from the two bodies. The force on the two bodies is determined by Lagrange’s energy method. This requires the total kinetic energy of the fluid and the two bodies, which is a function of the velocity potential that satisfies the boundary conditions at the surface of the bodies, and infinitely far away.

There are two cases to work out: motion in the line of centers, and motion perpendicular to it. Consider two identical spheres of radius  $a$ , as illustrated in Fig.1. Let  $\mathbf{U}$  be the velocity of sphere

$A$ , position  $\mathbf{x}$ , and let  $\mathbf{V}$  be the velocity of sphere  $B$ , position  $\mathbf{y}$ . Let  $M$  be the mass of each sphere, and  $M'$  be the corresponding mass of displaced fluid. Let  $\mathbf{c}$  be the vector pointing from  $A$  to  $B$  ( $\mathbf{c} = \mathbf{y} - \mathbf{x}$ ,  $c = |\mathbf{c}|$ ); with associated unit vector  $\hat{\mathbf{c}}$ . The general motion of each sphere can be split into two parts, one part that is parallel to the line of centers, and the other part which is not parallel. Let  $U_{\parallel} = \hat{\mathbf{c}} \cdot \mathbf{U}$ , so that  $\mathbf{U}_{\parallel} = \hat{\mathbf{c}} \hat{\mathbf{c}} \cdot \mathbf{U}$  is the parallel part, and let  $\mathbf{U}_{\perp} = \mathbf{U} - \mathbf{U}_{\parallel}$  be the perpendicular part of  $\mathbf{U}$ , and similarly for  $\mathbf{V}$ . Using this decomposition, equations of motion will be found using the energy method of Lagrange.

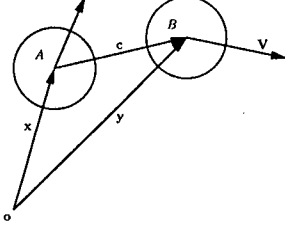


Figure 1. Two spheres in an arbitrary cartesian three space.

First, suppose that the motion is such that the velocity of both spheres is along the line of centers. The total energy of the fluid and the two spheres is [16]

$$T_{\parallel} = \frac{1}{2} [M + C_a M'] U_{\parallel}^2 - C_{\parallel} M' \mathbf{U}_{\parallel} \cdot \mathbf{V}_{\parallel} + \frac{1}{2} [M + C_a M'] V_{\parallel}^2 \quad (8)$$

where the coefficients  $C_a$  and  $C_{\parallel}$  are infinite series that arise from the potential flow solution for the velocity field. To obtain the fluid kinetic energy, the gradient of the velocity potential is squared, and integrated over all space. This is added to the sphere energies to yield the total energy. If the separation of centers is large, so that  $(a/c) \ll 1$ , it turns out that  $C_a = \frac{1}{2}$  and  $C_{\parallel} = \frac{3}{2}(a/c)^3$ . In order to examine close spacing, for which  $(a/c) \gg 1$ , a great many terms of series must be evaluated, which is done shortly.

If instead the motion is confined to be perpendicular to  $\mathbf{c}$ , the total energy is

$$T_{\perp} = \frac{1}{2} [M + C_a M'] U_{\perp}^2 + C_{\perp} M' \mathbf{U}_{\perp} \cdot \mathbf{V}_{\perp} + \frac{1}{2} [M + C_a M'] V_{\perp}^2 \quad (9)$$

In the large-spacing approximation,  $C_{\perp} = \frac{3}{4}(a/c)^3$  and again  $C_a = \frac{1}{2}$ . (In the perpendicular case for small spacing, both coefficients are not only different from these values, but very difficult to evaluate. Fortunately for the purposes of this paper, the evaluation is not needed, as will be seen shortly.)

Lagrange's equations, for the variation along  $\mathbf{x}$  (the trajectory of sphere  $A$ ) are

$$0 = \frac{d}{dt} \left( \frac{\partial T_{\parallel}}{\partial \mathbf{U}_{\parallel}} \right) - \nabla_{\mathbf{x}} T_{\parallel}, \quad 0 = \frac{d}{dt} \left( \frac{\partial T_{\perp}}{\partial \mathbf{U}_{\perp}} \right) - \nabla_{\mathbf{x}} T_{\perp} \quad (10a,b)$$

By carrying out the indicated differentiation, Lagrange's equations of motion are obtained. For this, the derivatives of the coefficients are needed. These are

$$\nabla_{\mathbf{x}} C_{\parallel} = \frac{\partial C_{\parallel}}{\partial \mathbf{x}} = \frac{dC_{\parallel}}{dc} \frac{\partial c}{\partial \mathbf{x}} = -C'_{\parallel} \hat{\mathbf{c}} \quad (11a)$$

and

$$\begin{aligned} \dot{C}_{\parallel} &= \frac{dC_{\parallel}}{dc} \dot{c} = C'_{\parallel} \hat{\mathbf{c}} \cdot (\dot{\mathbf{y}} - \dot{\mathbf{x}}) = C'_{\parallel} \hat{\mathbf{c}} \cdot (\mathbf{V} - \mathbf{U}) \\ &= C'_{\parallel} (V_{\parallel} - U_{\parallel}) \end{aligned} \quad (11b)$$

and likewise for  $C_a$ . Here the super prime signifies the derivative of the coefficient with respect to the spacing between centers  $c$ . Lagrange's equations are then

$$M (\mathbf{U}_{\parallel})' = -C_a M' (\mathbf{U}_{\parallel})' + M' \left[ (\mathbf{V}_{\parallel})' C_{\parallel} + V_{\parallel}^2 C'_{\parallel} \hat{\mathbf{c}} \right] \quad (12a)$$

$$M (\mathbf{U}_{\perp})' = -C_a M' (\mathbf{U}_{\perp})' - M' \left[ (\mathbf{V}_{\perp})' C_{\perp} + V_{\perp}^2 C'_{\perp} \hat{\mathbf{c}} \right] \quad (12b)$$

where the overdot again signifies the Lagrangian (total) derivative. This is a classical and well known result, and is obtained by assuming that  $C_a$  is a constant (independent of spacing  $c$ ). Recall that for the case of large spacing ( $a/c \ll 1$ ),  $C_{\parallel} = \frac{3}{2}(a/c)^3$  and  $C_{\perp} = \frac{3}{4}(a/c)^3$ . Hence  $C'_{\parallel} = -\frac{9}{2}(a^3/c^4)$  and  $C'_{\perp} = -\frac{9}{4}(a^3/c^4)$ . Now observe the right side terms in order, it is clear that: a) any acceleration is retarded by an amount proportional to that acceleration and the mass of displaced fluid; b) any acceleration of sphere  $B$  will cause an acceleration on  $A$  (and vice versa) that diminishes with increasing separation; and c) regardless of any accelerations, any motion in the line of centers, due to another sphere close by, will result in a force that lies in the line of centers; the parallel motion is repulsive and the perpendicular motion is attractive (because  $C'_{\parallel}$  and  $C'_{\perp}$  are negative). The first part is the usual added mass acceleration that a single isolated sphere would experience, the second part alters the first if the second sphere is also accelerating, and the third part acts as a repulsive-attractive force. [Two Remarks: 1) In the classical literature the quantity  $[M + C_a M']$  is called the "virtual mass"; and  $C_a M'$  is called the "added mass". 2) In the multiphase flow literature  $C_a$  is called the added mass coefficient, the value of which is very context dependent – a cause for both substantial confusion and lively debate.]

It is tempting to add the two equations of motion together in order to obtain the force associated with the fully *general* relative motion between the two bodies. Unfortunately there will be an error associated with this sum, because  $T_{\parallel} + T_{\perp}$  is not the actual total energy of the system. It is true that the velocity potentials are additive for the two cases (parallel and perpendicular motion), so the true fluid kinetic energy at a point is the gradient of the *combined* potential, squared. Hence adding the forces for the separate problems misses the cross term associated with squaring the combined velocity potential. It appears that the total fluid energy for the combined problems has not been computed (or at least does not appear in the accessible literature). Until the general (combined parallel and perpendicular) fluid energy is determined, we shall confine our attention to the restricted flow associated with fluidized beds. In this restricted case we shall suppose that the forces arising from two-body motions and accelerations that are perpendicular to the line of centers will simply average to zero.

In the 1-D approximation, the full equation of motion becomes, using Eq.(11) to express the result in terms of the directional gradient  $\nabla_{\mathbf{x}}$ ,

$$\begin{aligned} M (\mathbf{U}_{\parallel})' &= -M' \left[ C_a (\mathbf{U}_{\parallel})' - C_{\parallel} (\mathbf{V}_{\parallel})' \right] \\ &+ M' \left[ U_{\parallel} (V_{\parallel} - U_{\parallel}) + \frac{1}{2} (U_{\parallel}^2 + V_{\parallel}^2) \right] \nabla_{\mathbf{x}} C_a - M' V_{\parallel}^2 \nabla_{\mathbf{x}} C_{\parallel} \\ &+ M' C_a \nabla_{\mathbf{x}} \left[ U_{\parallel} (V_{\parallel} - U_{\parallel}) + \frac{1}{2} (U_{\parallel}^2 + V_{\parallel}^2) \right] - M' C_{\parallel} \nabla_{\mathbf{x}} V_{\parallel}^2 \end{aligned} \quad (13)$$

where the variation of  $C_a$  with spacing  $c$  is permitted. This is to be averaged with respect to the possible directions for the separation vector, the velocity, and the coefficients. For this we assume that the velocity is already a continuous (averaged) field, so that

$$\mathbf{V} = \mathbf{U} + \mathbf{c} \cdot \nabla \mathbf{U} \quad (14)$$

and let angle brackets signify the average *over directions*. Consider the term  $\langle \mathbf{U}_{\parallel} \rangle$  which is the variation of the parallel part of the velocity, along the center-of-mass motion, whose average is

$$\langle \langle \mathbf{U}_{\parallel} \rangle \rangle = \langle \hat{\mathbf{c}} \hat{\mathbf{c}} \cdot \dot{\mathbf{U}} + (\hat{\mathbf{c}} \hat{\mathbf{c}})' \cdot \mathbf{U} \rangle = \frac{1}{3} \dot{\mathbf{U}} \quad (15)$$

which assumes that the separation vector is isotropic, and time-independent. The factor  $\frac{1}{3}$  arises from the directional averaging, which is formally over the surface of a sphere of radius  $c$ , and outward normal  $\hat{\mathbf{c}}$  (See Landau & Lifshitz [17], footnote p. 79.) The next term is

$$-\langle C_{\parallel} (\mathbf{V}_{\parallel})' \rangle = -\frac{1}{3} C_{\parallel} \dot{\mathbf{U}} + \mathcal{O}(\nabla \mathbf{U})^2 \quad (18)$$

because  $C_{\parallel}$  does not involve the direction  $\mathbf{c}$ . However  $\nabla_{\mathbf{x}} C_{\parallel}$  explicitly depends on the direction, which is quite important in the directional averaging of the other terms. For these, we make the following association:

$$\nabla_{\mathbf{x}} C_{\parallel} \rightarrow \frac{dC_{\parallel}}{d\theta_s} \nabla \theta_s \quad (19)$$

which selects a specific direction – one associated with the gradient in volume fraction. This is equivalent to assuming that the *most probable* direction is that of increasing volume fraction of the spheres  $\theta_s$ , and the probability increases with its gradient. This is consistent with the assumption behind using Eq.(13) to obtain the full force vector: the perpendicular parts have averaged to zero. Hence it follows that

$$\begin{aligned} -\langle V_{\parallel}^2 \nabla_{\mathbf{x}} C_{\parallel} \rangle &= -\langle (\hat{\mathbf{c}} \cdot \mathbf{U} + \hat{\mathbf{c}} \cdot \mathbf{c} \nabla \cdot \mathbf{U})^2 \rangle \nabla_{\mathbf{x}} C_{\parallel} \\ &= -\langle (\hat{\mathbf{c}} \cdot \mathbf{U})^2 \rangle \nabla_{\mathbf{x}} C_{\parallel} + \mathcal{O}(\nabla \mathbf{U})^2 \\ &= -\frac{1}{3} U^2 \frac{dC_{\parallel}}{d\theta_s} \nabla \theta_s \end{aligned} \quad (20)$$

because the terms that are odd in  $\mathbf{c}$  average to zero, and a term proportional to the square of the velocity gradient is dropped. The derivative of the coefficient is evaluated later. [Remark: On the first line the directional derivative is removed from the averaging symbol because it is being held fixed; it is a known quantity by way of Eq.(19). This is a departure from standard practice, the consequences of which will be shown soon.] Similarly the next term, averaged over directions, is

$$\left\langle \left[ U_{\parallel} (V_{\parallel} - U_{\parallel}) + \frac{1}{2} (U_{\parallel}^2 + V_{\parallel}^2) \right] \nabla_{\mathbf{x}} C_a \right\rangle = \frac{1}{3} U^2 \frac{dC_a}{d\theta_s} \nabla \theta_s \quad (21)$$

plus a term of order  $(\nabla \mathbf{U})^2$ . The last two terms will be taken together, and averaged in the same way; the result is important because it happens to have the largest coefficients. The average

takes four steps, and makes use of the constant direction vector, in unit form  $\hat{\mathbf{a}} = \nabla \theta_s / |\nabla \theta_s|$ . The steps are

$$\begin{aligned} &\left\langle C_a \nabla_{\mathbf{x}} \left[ U_{\parallel} (V_{\parallel} - U_{\parallel}) + \frac{1}{2} (U_{\parallel}^2 + V_{\parallel}^2) \right] - C_{\parallel} \nabla_{\mathbf{x}} V_{\parallel}^2 \right\rangle \\ &= 2(C_a - C_{\parallel}) \langle U_{\parallel} \nabla_{\mathbf{x}} U_{\parallel} \rangle + \mathcal{O}(\nabla \mathbf{U})^2 \\ &= 2(C_a - C_{\parallel}) \langle (\hat{\mathbf{c}} \cdot \mathbf{U}) \cdot (\hat{\mathbf{a}} \hat{\mathbf{a}} \cdot \nabla) (\hat{\mathbf{c}} \cdot \mathbf{U}) \rangle \\ &= 2(C_a - C_{\parallel}) \langle \hat{\mathbf{c}} \hat{\mathbf{c}} \rangle \mathbf{U} \cdot (\hat{\mathbf{a}} \hat{\mathbf{a}}) \cdot \nabla \mathbf{U} \\ &= \frac{2}{3} (C_a - C_{\parallel}) \mathbf{U} (\nabla \cdot \mathbf{U}) . \end{aligned} \quad (22)$$

There are four steps shown, corresponding to the four right-side terms. The first step uses the velocity expansion, eliminates odd terms in  $\hat{\mathbf{c}}$  (which average to zero), and expands the directional derivative. The second step uses the definition of  $U_{\parallel}$  and expresses the gradient in terms of the direction tensor  $\hat{\mathbf{a}} \hat{\mathbf{a}}$ . The third step removes the velocity and its gradient from the averaging symbol, because they have already been averaged. The last step performs the average, and eliminates the directional tensor because it is just the identity tensor in the 1-D approximation, whereby the divergence is used to obtain a symmetric form in the gradient.

Hence Lagrange's equation of motion for sphere  $A$ , averaged assuming a linear distribution of sphere velocity becomes, to lowest order in the velocity gradient,

$$\begin{aligned} M \dot{\mathbf{U}} &= - (C_a - C_{\parallel}) M' \dot{\mathbf{U}} \\ &\quad + \frac{d}{d\theta_s} (C_a - C_{\parallel}) M' U^2 \nabla \theta_s \\ &\quad + 2 (C_a - C_{\parallel}) M' \mathbf{U} (\nabla \cdot \mathbf{U}) \end{aligned} \quad (23)$$

The right side is the total force on a body moving in a sea of fluid whose averaged velocity is zero. For a sea of perfect fluid whose averaged velocity is nonzero, say  $\mathbf{u}_f$ , it is common practice to replace  $\mathbf{U}$  with  $\mathbf{u}_s - \mathbf{u}_f$  where  $\mathbf{u}_s$  is the ensemble-averaged velocity of the dispersed (in this case, solid) field. In developing the standard force it was assumed that each individual body contributes to the ensemble average the same amount of force, so the force density is simply the number density  $n = \theta_s / V_s$  (volume fraction per volume of one sphere) times the force for a single body; the same assumption is made here. With these provisions, the force density acting on the  $s$ -field due to motion relative to the  $f$ -field, is

$$\begin{aligned} \mathbf{f}_{sf} &= -\theta_s (C_a - C_{\parallel}) \rho_f^o (\dot{\mathbf{u}}_s - \dot{\mathbf{u}}_f) \\ &\quad + \theta_s \frac{d}{d\theta_s} (C_a - C_{\parallel}) \rho_f^o (u_s - u_f)^2 \nabla \theta_s \\ &\quad + 2 (C_a - C_{\parallel}) \rho_f^o (\mathbf{u}_s - \mathbf{u}_f) (\theta_s \nabla \cdot \mathbf{u}_s) \end{aligned} \quad (24)$$

In keeping with standard practice, we apply a factor of  $\theta_f$  to the first term, which can be thought of as discounting the acceleration-dependent added mass acceleration because of the presence of a mean pressure gradient (which already has the large-scale part of the added mass effect in it). Also the fluid field may have gradients that are independent from the dispersed field, and which can cause forces to arise even in the absence of gradients in the dispersed field. For this reason we add a factor of  $\theta_f (\nabla \cdot \mathbf{u}_f)$  to the third right-side term. This permits combination of the second two terms, by using the canonical identity

$$\theta_s (\nabla \cdot \mathbf{u}_s) + \theta_f (\nabla \cdot \mathbf{u}_f) = -(\mathbf{u}_s - \mathbf{u}_f) \nabla \theta_s . \quad (25)$$

Now let  $\rho_{sf}^o$  be the material density of the “continuous” field (in this case the f-field), and let  $\theta_d$  be the volume fraction of the “dispersed” field. The expression for the two-body potential flow force becomes

$$\mathbf{f}_{sf} = -\theta_s \theta_f \tilde{C}_a \rho_{sf}^o (\dot{\mathbf{u}}_s - \dot{\mathbf{u}}_f) - \tilde{C}_r \rho_{sf}^o (u_s - u_f)^2 \nabla \theta_s \quad (26a)$$

where the net coefficients, signified by the over-tilde, are

$$\tilde{C}_a = (C_a - C_{||}) , \quad (26b)$$

$$\tilde{C}_r = 2 (C_a - C_{||}) - \theta_d \frac{d}{d\theta_d} (C_a - C_{||}) . \quad (26c)$$

Equation (26) is now a force density that is “symmetric” in the material indices. That is, the force on the f-field due to interaction with the s-field is obtained by interchanging the indices f and s. Because  $\nabla \theta_f = -\nabla \theta_s$  the force is equal and opposite, and  $\mathbf{f}_{sf} + \mathbf{f}_{fs} = 0$  as is required by the exchange force. The net coefficients  $\tilde{C}_a$  and  $\tilde{C}_r$  are both positive for all values of  $\theta_d$ , as will be shown next. Hence  $\tilde{C}_a$  is an added mass coefficient, and  $\tilde{C}_r$  multiplies a term that represents a net repulsive force.

Positivity of the net coefficients is shown by observing the behavior of the potential flow problem, with unrestricted spacing between the two spheres. Recall that  $C_a$  and  $C_{||}$  are both sums arising from the infinite series solution for the velocity potential. As sphere separation decreases,  $C_a$  and  $C_{||}$  (and their derivatives with respect to spacing) must be modified by a factors that reflect higher order disturbances in one sphere’s potential flow field introduced by the other sphere. The evaluation of these factors requires the truncation of the infinite series. By extending the prescription for generating these infinite series outlined by Lamb [16], correction factors can be produced that, in principle, extend in validity up to the point where the spheres are touching. If one hundred terms are retained in each of the series for  $C_a$  and  $C_{||}$ , one can reduce the error in the analytic results to less than 0.01 percent for both series [18].

In order to produce a tractable model that includes the physics of close-spacing, a set of fits to the infinite series is used. (Because the derivatives are singular when the spheres come into contact, the finite number of terms kept here only serves to guide the fit when the separation gap approaches zero.) The natural variable for expressing the fits is the quantity  $\xi = (c - 2a)/a$ , which is the distance between sphere surfaces (the gap) expressed in sphere radii. We shall refer to  $\xi$  as the “separation number”, which varies from zero to infinity. The fits used here are

$$C_a = \frac{1}{2} + \frac{3}{2} [(\xi + 1)(\xi + 3)]^{-3} (1 + 0.294e^{-7.69\xi}) , \quad (27a)$$

$$C_{||} = \frac{3}{2} (\xi + 2)^{-3} (1 + 0.160e^{-5.75\xi}) , \quad (27b)$$

$$\frac{d}{d\xi} (C_a - C_{||}) = \frac{9}{2} (\xi + 2)^{-4} (1 - 0.428e^{-1.31\xi}) . \quad (27c)$$

Note that the corrections to  $C_a$  and  $C_{||}$  small, and occur at  $\xi = 0$  where the spheres are touching. [Remark: The infinite series are analytic at  $\xi = 0$ , and are expressible in terms of the Riemann  $\zeta$ -function. The difference between the fits and the analytic values is very small.]

Now recall that we really need the derivative with respect to the volume fraction. This requires a modeling step, and the chain rule from calculus. Hence we use

$$\frac{d}{d\theta_d} (C_a - C_{||}) = \left( \frac{d\xi}{d\theta_d} \right) \frac{d}{d\xi} (C_a - C_{||}) . \quad (28)$$

So last thing needed here is to relate the separation number  $\xi$  to the dispersed field volume fraction. For regular arrays of spheres, this can be transformed *exactly* into a function of  $\theta_d$  and the volume fraction at closepacking  $\theta_{cp}$ . It turns out that

$$\xi = \frac{c}{a} + 2 \equiv 2 \left[ (\theta_{cp}/\theta_d)^{\frac{1}{k}} - 1 \right] = \xi(\theta_d) \quad (29)$$

where  $k$  is the dimensionality;  $k = 3$  corresponds to a cubic array of spheres,  $k = 2$  is a 2-D array of spheres in a plane, and  $k = 1$  is a 1-D line of spheres. (In 2-D the depth of fluid normal to the plane, and in 1-D the radius of fluid normal to the line, both factor out because  $\theta_d$  and  $\theta_{cp}$  both depend on the same arbitrary dimension.)

For  $k = 3$ ,  $\theta_{cp} = \pi/6 \approx 0.524$  (a bit smaller than random close-packed uniform spheres, for which  $\theta_{cp} \approx 0.644$ ). To furnish a quantitative feel for the separation number,  $\xi(\theta_d)$  is plotted in Fig.2, for  $k = 1, 2, 3$ . Figure 2a shows  $\xi$  for  $\theta_d$  down to one percent. Figure 2b displays the range  $10^{-8} < \theta_d < 10^{-2}$ .

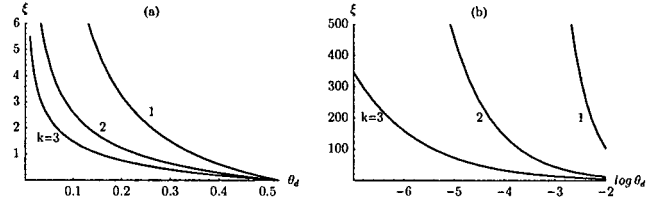


Figure 2. Separation number  $\xi(\theta_d)$  for  $k = 1, 2, 3$ .

The main point of this figure is to show that the separation number exhibits a strong dependence on the dimensionality  $k$ . At large separation, the multibody effects vanish. A separation number of 200 radii is 100 diameters; this occurs, roughly, at values of volume fraction of  $< 10^{-6}$ ,  $< 10^{-4}$  and  $< 10^{-2}$  for  $k = 3, 2, 1$  respectively. The modeling performed in this paper is to generalize 1-D forces into multidimensional ones – a process that leaves  $k$  uncertain. For this reason, we shall leave the dimensionality as a parameter, lying somewhere in the physical range  $1 \leq k \leq 3$ , that is yet to be determined. Because the fits in Eq.(27) are all decaying exponentials the nonviscous behavior is insensitive to  $k$ ; however the corresponding fit for the viscous force can depend strongly on  $k$ , as will be seen in the next section.

Finally the net coefficients can be displayed as functions of  $\theta_d$ . Using Eq.(29) the net repulsive coefficient becomes

$$\tilde{C}_r = 2 (C_a - C_{||}) + \left( \frac{\xi + 2}{k} \right) \frac{d}{d\xi} (C_a - C_{||}) \quad (26d)$$

where we retain the unspecified dimensionality  $k$ . Figure 3 shows both of the net coefficients, plotted for  $k = 1, 2, 3$ . The important point here is that these coefficients are nonnegative for all values of  $\theta_d$ , right up to the point of close-packing. [Two remarks: 1) Holding the directional derivative fixed while averaging over directions is a crucial feature of the foregoing procedure. If the directional derivative is *not* held fixed the model is fully isotropic, and the net repulsive coefficient  $\tilde{C}_r$  is (3/5) times smaller. 2) It

is the net coefficients that are important here; they go together hand-in-hand.]

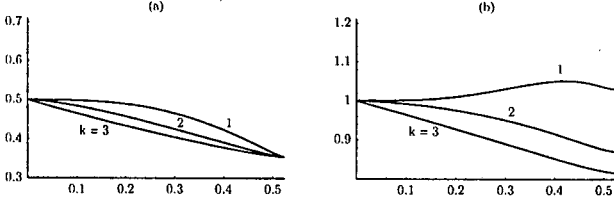


Figure 2. Net coefficients. (a)  $\tilde{C}_\alpha(\theta_d)$ , (b)  $\tilde{C}_r(\theta_d)$ .

## 5. THE TWO-BODY VISCOUS FLOW FORCE

The contribution to  $\mathbf{f}_{rs}$  that is due to the motion of one body relative to another in a viscous fluid, is included here. The force contribution is a multidimensional generalization of the zero Reynolds number 1-D force, developed by Batchelor & Green [14], averaged. For two identical spheres moving in the line of centers, the force on one sphere is, using the nomenclature of [14]

$$F_z = -\frac{3}{2}\pi\mu a V_z h_v(\xi) \quad (30a)$$

where the function is

$$h_v(\xi) = [\xi^{-1} + \frac{9}{10}\log(\xi^{-1}) + 2.763] \quad (30b)$$

which becomes singular at  $\xi = 0$ . (A term proportional to a constant fluid straining is not needed here, and is therefore omitted.) This is accurate for  $\xi \ll 1$  where again  $\xi = (c - 2a)/a$  is the separation number;  $F_z$  is the total force on one sphere in the  $z$ -component direction,  $\mu$  the fluid viscosity,  $a$  is the sphere radius,  $V_z$  is the relative velocity between spheres (confined to the  $z$  axis). As before,  $c$  is the distance between sphere centers. The line of centers coincides with the  $z$  axis.

This force is also known classically. The viscous force acts in such a direction to resist the relative motion of the two spheres; it is the reason that two bodies falling in a viscous fluid will tend to remain the same distance apart. [Two remarks: 1) Any motion perpendicular to the line of centers tends to make the spheres spin, because the total rotational moment is zero; the spheres spin in opposite directions (like a pair of gears). Hence the falling spheres may orbit one another at a fixed distance, while rotating in opposite directions. 2) The classical streaming viscous force, due to Stokes, is  $-6\pi\mu a \mathbf{V}$  where  $\mathbf{V}$  is the velocity of a sphere relative to a uniform fluid; this part is already included as part of the standard force. The force given in Eq.(30), due to relative motion between two identical spheres, is an additional one.]

The function  $h_v$  in Eq.(30b) is a fit to an infinite series, accurate for  $\xi \ll 1$  which corresponds to large  $\theta_d$  (near close-packing). For this paper it will be assumed valid for all  $\theta_d$ , but with unknown dimensionality  $k$ .

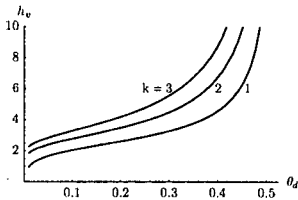


Figure 4. The function  $h_v[\xi(\theta_d)]$ .

Figure 3 displays  $h_v[\xi(\theta_d)]$  for  $k = 1, 2, 3$ , where it is clear that a low-dimensionality  $k = 1$  permits the viscous effect to diminish much faster as the volume fraction diminishes from  $\theta_{cp}$ , where the effect is infinite.

The task now is to place Eq.(30a) in general coordinates, and average. Consider sphere  $A$  in Fig.1; its velocity relative to  $B$  is  $-\mathbf{c} \cdot \nabla \mathbf{U}$ , whose projection in the line of centers is  $-\hat{\mathbf{c}} \cdot \mathbf{c} \cdot \nabla \mathbf{U}$ . As before we assume that  $\mathbf{U}$  is continuous, and therefore already averaged. Hence in general coordinates the force *magnitude* is

$$F = \frac{3}{2}\pi\mu a h_v c \hat{\mathbf{c}} \cdot \hat{\mathbf{c}} \cdot \nabla \mathbf{U} \quad (31)$$

Now average, assuming isotropic  $\hat{\mathbf{c}}$ , as in the previous section, and identify  $\mathbf{U}$  with the averaged velocity of the sphere field  $\mathbf{u}_s$ . Let us suppose that the direction of action is  $\pm(\mathbf{u}_s - \mathbf{u}_f)$ , which is along the mean relative velocity between fields; the correct sign will be chosen in the last step. (Choosing this direction assumes that the sphere-sphere relative velocity and the sphere-fluid relative velocity are similar.) The force vector becomes

$$\mathbf{F} = \pm [\frac{1}{2}\pi\mu a c/w] h_v(\mathbf{u}_s - \mathbf{u}_f) \nabla \cdot \mathbf{u}_s \quad (32)$$

where  $w = |\mathbf{u}_s - \mathbf{u}_f|$ . As before the force density  $\mathbf{f}_{sf}$  is  $n\mathbf{F}$ , with  $n = \theta_s/V_s$ . The coefficient in square brackets is cast in terms of the relative Reynolds number  $Re = wd/\rho_f^0\mu$  (based on diameter  $d = 2a$ ). The result is

$$\mathbf{f}_{sf} = \pm \theta_d C_v h_v \rho_{sf}^0 (\mathbf{u}_s - \mathbf{u}_f) \nabla \cdot \mathbf{u}_s \quad (34)$$

where the coefficient

$$C_v = [\frac{3}{4}(c/a)Re^{-1}] = [\frac{3}{4}(\xi + 2)Re^{-1}] \approx [\frac{3}{2}Re^{-1}] \quad (35)$$

is accurate only for  $Re \ll 1$ . The approximation on  $\xi$  is made because the Eq.(30) is accurate only for separation number  $\xi \ll 1$ . [Important remark: Because significant relative motion can only occur when the Reynolds number exceeds about one, multifield problems will typically have  $Re > 1$ . This means that some empiricism will be needed for determining  $C_v$ , which takes some of the pressure off from not knowing  $k$ .] Again because the background fluid may have gradients that generate a force, we add the factor  $\theta_f(\nabla \cdot \mathbf{u}_f)$  and use the identity in Eq.(nn) to place the force in terms of  $\nabla \theta_s$ . Let  $\mathbf{w}_{sf} = \mathbf{u}_s - \mathbf{u}_f$  and the viscous force becomes

$$\mathbf{f}_{sf} = -\text{sign}[\mathbf{w}_{sf} \cdot \nabla \theta_s] C_v h_v \rho_{sf}^0 (\mathbf{w}_{sf} \mathbf{w}_{sf} \cdot \nabla \theta_s) \quad (35)$$

where the first factor makes the direction definite (the sign function has a unit value times the sign of its argument). The direction is chosen so that the averaged equation has the same attractive-repulsive nature that the single-body force had to begin with. In the one dimensional fluidized bed waves, described in the Introduction, the expansion wave has a positive vertical gradient of solids volume fraction, and  $\mathbf{u}_s - \mathbf{u}_f$  is negative. The foregoing force acts upward, and therefore it appears that the grains are attracting one another as they are pulling apart. Conversely in the compression wave the vertical component of  $\nabla \theta_s$  is negative while the relative velocity is also negative. The force again acts upward, so the grains appear to be repulsive to one another as they

are coming closer together. Note that if the relative velocity is perpendicular to  $\nabla\theta_s$ , the force is zero.

This force contributes a destabilizing term in the expansion case. That is, a volume fraction gradient that is positive produces a force that is positive – which acts to increase the gradient. In the case of compression the force is stabilizing because the force acts in order to diminish the volume fraction gradient.

Now observe that  $\mathbf{f}_{sf}$  is in the symmetric form that is desirable for general use; the interchange of s–f indices gives the force on the f–field due to interaction with s–field, and  $\mathbf{f}_{sf} + \mathbf{f}_{fs} = 0$ . To summarize, the full force density used in the studies that follow, is

$$\mathbf{f}_{sf} = -\theta_s\theta_f\tilde{C}_a\rho_{sf}^o(\dot{\mathbf{u}}_s - \dot{\mathbf{u}}_f) - \tilde{C}_r\rho_{sf}^o w_{sf}^2 \nabla\theta_s - \tilde{C}_v h_v \rho_{sf}^o (\mathbf{w}_{sf} \mathbf{w}_{sf} \cdot \nabla\theta_s) - \theta_s\theta_f \mathcal{K}_{sf} \mathbf{w}_{sf} \quad (36a)$$

where the potential flow lift force is omitted because we are interested only in the 1–D case, and the net viscous coefficient is

$$\tilde{C}_v = \text{sign}[\mathbf{w}_{sf} \cdot \nabla\theta_s] C_v \quad (26b)$$

which simply absorbs the sign into the unknown coefficient  $C_v$ .

## 6. CHARACTER OF THE 1-D EQUATIONS

The character of the 1-D model equations, using only the standard force, is well known [2,10,11,19,20]. The eigenvalues of the characteristic equation are complex, so the equation system is said to be illposed, in the mathematical sense. Stewart & Wendroff [10] comment that illposed problems are difficult, but not impossible, in the context of two–phase flow. Indeed this has been the case; a great deal of useful analysis has been accomplished with the standard force, in a large collection of problems. For the study of waves in fluidized beds the illposedness has slowed the progress, but not stopped it altogether [1]. Nevertheless a well–posed model is helpful for the study of waves because real–valued eigenvalues permit analytic solutions to be found for the wave speeds and wave structures. The main purpose of this section is to demonstrate that the addition of a two–body potential flow force is sufficient to guarantee real eigenvalues, unconditionally.

Let us first consider the two–field case, and postpone the study of three or more fields for future work. Let the state vector be  $V = [\rho_1, \rho_2, u_1, u_2, p]^T$ , and let  $w_{12} = u_1 - u_2$ , with  $x$  the single coordinate direction. The force density acting on field 1 due to interaction with field 2 is, from the summary of the last section,

$$f_{12} = -\theta_1\theta_2\tilde{C}_a\rho_{12}^o(\dot{u}_1 - \dot{u}_2) - (\tilde{C}_r + \tilde{C}_v h_v)\rho_{12}^o w_{12}^2 (\theta_1)_x - \theta_1\theta_2 \mathcal{K}_{12} w_{12} \quad (37)$$

The corresponding 1–D model equations, expressed in matrix form, are

$$\mathbf{A}V_t + \mathbf{B}V_x = \mathbf{S} \quad (38a)$$

where

$$\mathbf{A} = \begin{bmatrix} 1 & 0 & 0 & 0 & 0 \\ 0 & 1 & 0 & 0 & 0 \\ 0 & 0 & \rho_1 + A & -A & 0 \\ 0 & 0 & -A & \rho_2 + A & 0 \\ v_1 & v_2 & 0 & 0 & 0 \end{bmatrix} \quad (38b)$$

$$\mathbf{B} = \begin{bmatrix} u_1 & 0 & \rho_1 & 0 & 0 \\ 0 & u_2 & 0 & \rho_2 & 0 \\ Bv_1 & 0 & (\rho_1 + A)u_1 & -Au_2 & \theta_1 \\ 0 & Bv_2 & -Au_1 & (\rho_2 + A)u_2 & \theta_2 \\ 0 & 0 & 0 & 0 & 0 \end{bmatrix} \quad (38c)$$

and the right side vector is

$$\mathbf{S} = \begin{bmatrix} 0 \\ 0 \\ -\theta_1\theta_2\mathcal{K}w_{12} + \rho_1 g \\ +\theta_1\theta_2\mathcal{K}w_{12} + \rho_2 g \\ 0 \end{bmatrix} \quad (38d)$$

The dummy variables are

$$A = \theta_1\theta_2\tilde{C}_a\rho_{12}^o, \quad B = (\tilde{C}_r + \tilde{C}_v h_v)w_{12}^2\rho_{12}^o \quad (38e,f)$$

and

$$\theta_1 = \rho_1 v_1, \quad \theta_2 = \rho_2 v_2, \quad v_1 = 1/\rho_1^o, \quad v_2 = 1/\rho_2^o. \quad (38g,h,i,j)$$

The densities  $(\rho_1 + A)$  and  $(\rho_2 + A)$  could be called virtual mass densities, for each field, and the density  $A$  could be called an added mass density. Because the material specific volumes are constant, this is a complete set of equations. The corresponding characteristic equation is  $\text{Det}[\mathbf{B} - \lambda\mathbf{A}] = 0$ , which turns out to be quadratic in the eigenvalues  $\lambda$ . The eigenvalues are exactly analogous to “characteristic speeds” in gas dynamics. Let field 1 be the continuous field, so that  $\rho_{12}^o = \rho_1^o$ . The eigenvalues are

$$\lambda = u_1 - w_{12} \left( \beta \pm \sqrt{D[\theta_2(1 + \tilde{C}_a) + \theta_1(\gamma + \tilde{C}_a)]} \right) \quad (39a)$$

where  $\gamma = \rho_2^o/\rho_1^o$  is the material density ratio of dispersed to continuous fields, and in which

$$\beta = \theta_1(\gamma + \tilde{C}_a)/[\theta_2(1 + \tilde{C}_a) + \theta_1(\gamma + \tilde{C}_a)] \quad (39b)$$

is a positive number whose value lies between zero and one; because  $\tilde{C}_a$  is always near  $\frac{1}{2}$ ,  $\beta$  depends only on the density ratio  $\gamma$  and the volume fractions. The factor  $D$ , which must be positive if the eigenvalues are to be real, is

$$D = (\tilde{C}_r + \tilde{C}_v h_v) - \frac{\theta_1\theta_2}{[\theta_1/(1 + \tilde{C}_a)] + [\theta_2/(\gamma + \tilde{C}_a)]} \geq 0. \quad (39c)$$

The character of the equations can be observed by plotting  $D$ . Consider the nonviscous case first. Figure 5 shows  $D$  for  $k = 3$ , and various values of the ratio of material density  $\gamma$ ; and for two values of  $\theta_{cp}$ . For  $\theta_{cp} = \pi/6 \approx 0.524$ , appropriate for the coefficients derived here,  $D$  is positive for all values of  $\theta_d$  and  $\gamma$ , so it is possible to conclude that the nonviscous equations are unconditionally hyperbolic. This is true for values of  $k = 2$  and  $k = 1$  as well. For  $\theta_{cp}$  somewhat greater than  $\pi/6$ , and for which the coefficients are *not* appropriate, the large  $\gamma$  case can exhibit negative  $D$ ; the significance of this will be discussed shortly.

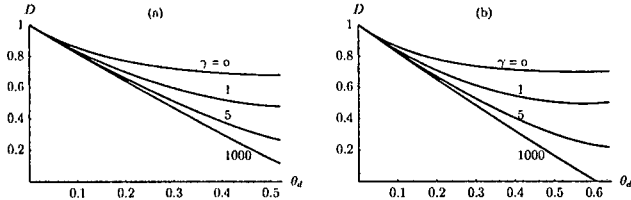


Figure 5.  $D$  for  $C_v = 0$ . (a)  $\theta_{cp} = 0.524$ , (b)  $\theta_{cp} = 0.644$ .

Now let us consider addition of the viscous attractive–repulsive force, and its corresponding effect on the system character. Recall that the direction of action is given by  $\text{sign}[w_{12}(\theta_1)_x]$  which is positive in the case of a compression wave; in the expansion wave the coefficient is negative. The analytic magnitude of  $\tilde{C}_v \approx Re^{-1}$  is only valid for  $Re \ll 1$ , and so for practical conditions this coefficient is an unknown parameter. Its value, in relation to all of the other modeling assumptions associated with the drag force and added mass force, can only be grossly estimated, as follows. Figure 6 displays the condition  $D$ , plotted versus dispersed field volume fraction, for two cases: a)  $\tilde{C}_v = +0.01$  (compression); and b)  $\tilde{C}_v = -0.01$  (expansion).

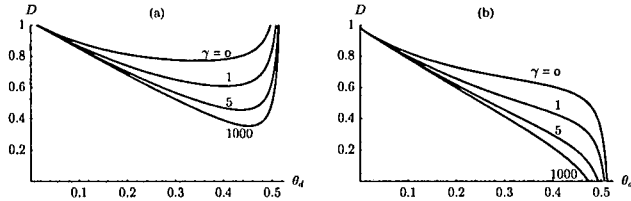


Figure 6.  $D$  for  $\theta_{cp} = 0.524$ . (a)  $C_v = +0.01$ , (b)  $C_v = -0.01$ .

In Fig. 6, the volume fraction at close packing is again  $\theta_{cp} = 0.524$  corresponding to rigid uniform spheres in a regular cubic array. In the compression case  $D$  is positive, and becomes large near close-packing, which is to be expected because the viscous force is stable in compression waves. In the expansion case  $D$  becomes negative near close-packing; because the function  $h_v$  becomes infinite at  $\theta_{cp}$ ,  $D$  will be negative there for *any* negative  $C_v$ , regardless of the magnitude of  $C_v$ .

Recall that when the bed of grains becomes close-packed, the configuration stress is nonzero (Sec.3). This brings in a large positive contribution to  $D$  that is not included here, but the effect is to produce 1-D wave speeds that depend on the elasticity of the grains themselves. So the issue with negative  $D$  near  $\theta_{cp}$  becomes a question of how the state in a packed bed can transition to smaller values of  $\theta_d$  in an expansion wave, by passing over those states for which  $D$  is negative. The answer is that such a transition can only occur through a discontinuity of  $\theta_d$ , so the expansion wave takes on a compound structure. The compound structure is a discontinuity from  $\theta_{cp}$  to some lower value, after which the wave is smooth, and travels with the speed of an eigenvalue. Which eigenvalue will depend on the value of  $C_v$ ; for this reason, the data from Wallis *et al.* [1] is extremely important. Those data permit an experimental determination of the coefficient that is not possible to determine from theory alone, at least at the present time.

Because solutions to the 1-D wave problems depend on the eigenvalues, additional insight into the physical wave behavior can be gained by observing  $\lambda$  in certain limits. The main observation is that the behavior always depends on the magnitude of  $\gamma$  compared to the net added mass coefficient  $\tilde{C}_a$ . Recall that  $\gamma$

is the ratio of dispersed to continuous material density; so  $\gamma$  is small for gas bubbles in liquid, of order one for solid grains in liquid, and very large for solid grains in a gas. Now consider the infinitely dilute limit, for which  $\theta_d \rightarrow 0$ ,  $\beta \rightarrow 1$ ,  $D \rightarrow 1$ , and the relative velocity becomes the terminal velocity  $w_T$ . Thus  $\lambda = u_1 - w_T[1 \pm (\gamma + \tilde{C}_a)^{1/2}]$ . For small  $\gamma$  (gas-in-liquid) the  $\lambda$  will be similar to the fluid velocity, plus or minus the terminal velocity. For large  $\gamma$  (solid-in-gas) the dilute eigenvalues can become very large relative to the fluid velocity. Not surprisingly, this means that expansion waves can travel very fast when the fluid is light compared to the dispersed material.

Near the close-packing limit, the value volume fraction is always near  $\frac{1}{2}$ . Now the relative velocity is much smaller than the terminal velocity, and is related to the minimum fluidization velocity and the value of  $\theta_{cp}$ . For small  $\gamma$  the wave speeds are still not far from the fluid velocity. For large  $\gamma$ ,  $\beta \rightarrow 0$ , so that  $\lambda = u_1 \pm w_T(D\gamma)^{1/2}$ . The large- $\gamma$  value of  $D$  near close packing is always small in expansion waves. This means that conditions can exist for which the square root evaluates to one, and because  $u_1$  is also like  $w_T$ , one of the eigenvalues can tend toward zero. If this corresponds to the direction of the expansion wave, it means that the expansion wave will come to rest relative to the region where the bed is packed. This nature of the expansion wave explains the very unstable (and well known) behavior grain beds fluidized with gas, compared to the more stable behavior of grain beds fluidized with liquid.

## 7. SUMMARY

A study of two-body forces due to both inertial (potential flow) and viscous (Stokes flow) effects has yielded multifield model equations that exhibit features that are new. The model is low-order because gradients that generate the two-body forces are linear, time-independent, and one-dimensional. The nonviscous model is shown to be unconditionally hyperbolic; a feature that is helpful for developing analytic solutions for 1-D wave problems, and for ensuring physical statistics from three-dimensional LES results used for turbulence closures. The viscous force acts in such a way that an expanding fluidized bed appears to have grains attracted to one another. This attractive force gives the expanding bed a sort of “strength” that must be overcome in order to expand. If the magnitude is large enough, the attraction will slow the expansion wave at the packed bed limit, and could bring the wave to rest relative to the packed bed.

The next step is to find the analytic solutions for 1-D nonviscous, and viscous problems. In the viscous case, experimental data are needed in order to gauge one of the coefficients in the new model. The data from Wallis, *et al.* [1] will serve that purpose well. After that a higher-order model could be developed by considering fully general relative motions between two grains in the potential flow problem. This should lead to a two-body correction to the potential-flow lift force found by Drew & Lahey [8]; and the hyperbolic character of the 1-D nonviscous model should remain.

## NOMENCLATURE

$A$  – like  $B$ ,  $U$ ,  $x$ ,  $\mathbf{x}$ ,  $\mathbf{U}$  . . . , the Roman alphabet, in both plain and bold face, is used for dummy variables defined locally in the text.

$a$  – sphere radius [length]  
 $c$  – distance between sphere centers [length]  
 $d$  – sphere diameter [length]  
 $f$  – force density [force/volume]  
 $g$  – gravity component [velocity/time]  
 $h$  – close-spacing function [nondimensional]  
 $n$  – number density [number/volume]  
 $p$  – hydrodynamic pressure [force/area]  
 $q$  – derivative close-spacing function [nondimensional]  
 $t$  – time  
 $u$  – velocity component [length/time]  
 $v$  – specific volume [volume/mass]  
 $w$  – relative velocity component [length/time]  
 $x$  – coordinate component [length]  
 $z$  – coordinate component [length]  
 $C$  – nondimensional coefficient  
 $\mathcal{H}$  – Saffman's function (nondimensional)  
 $Re$  – Reynolds number based on the mean relative velocity, sphere diameter, and fluid properties (nondimensional)  
 $\mathbf{c}$  – vector from sphere A center to sphere B center [length]  
 $\mathbf{f}$  – force density [force/volume]  
 $\mathbf{g}$  – acceleration due to gravity [velocity/time]  
 $\mathbf{u}$  – velocity [length/time]  
 $\mathbf{w}$  – relative velocity [length/time]  
 $\mathbf{x}$  – position [length]  
 $\mathbf{y}$  – position [length]  
 $\mathbf{I}$  – the identity tensor [nondimensional]  
 $\mathbf{R}$  – Reynolds stress [force/mass]  
 $\mathbf{U}$  – velocity of sphere at position  $\mathbf{x}$ , called  $A$   
 $\mathbf{V}$  – velocity of sphere at position  $\mathbf{y}$ , called  $B$   
 $\rho$  – mass density [mass/volume]  
 $\theta$  – volume fraction [nondimensional]  
 $\mu$  – viscosity [mass/length/time]  
 $\xi$  – separation gap in sphere radii [nondimensional]  
 $\sigma$  – stress [force/area]

#### Subscripts, superscripts, and over-symbols

$( )_a$  – having to do with added mass  
 $( )_d$  – having to do with the dispersed material field  
 $( )_o$  – a point in space-time ( $\mathbf{x}, t$ )  
 $( )_r$  – integer material index  
 $( )_r$  – having to do with a repulsive force  
 $( )_v$  – having to do with viscosity  
 $( )_{||}$  – parallel  
 $( )_{\perp}$  – perpendicular  
 $( )$  – The Lagrangian (material) derivative, sometimes  $( )^*$  for clarity of the operator, if the operand is a compound quantity.  
 $( \hat{ } )$  – a unit vector  
 $( )'$  – a dummy symbol for: a fluctuation, a derivative, or mass of displaced fluid (defined in the text).

#### ACKNOWLEDGMENTS

This work is supported by the U. S. Department of Energy, under contract W-7405-ENG-36.

#### REFERENCES

1. G. B. Wallis, S. P. Harvey, & R. Di Felice, Decompression Waves in Fluidized Beds, *Int. J. Multiphase Flow*, vol. 19, pp. 839–874, 1993.
2. D. A. Drew, G. S. Arnold, & R. T. Lahey, Jr., Relation of Microstructure to Constitutive Equations, in D. D. Joseph & D. G. Schaeffer (eds.), *Two Phase Flows and Waves*, p. 45, Springer-Verlag, New York, 1990.
3. D. Lhuillier, The Macroscopic Modelling of Multi-Phase Mixtures, in U. Schafinger (ed.), *Flow of Particles in Suspensions*, p. 39, Springer-Verlag, Vienna, 1996.
4. B. A. Kashiwa & R. M. Rauenzahn, A Multimaterial Formalism, in *Numerical Methods in Multiphase Flows*, p. 149, FED-Vol. 185, ASME, New York, 1994.
5. P. G. Saffman, On the Boundary Condition at the Surface of a Porous Medium, *Studies in Appl. Math.*, vol. 50, pp. 93–101, 1971.
6. G. B. Wallis, *One-dimensional Two-phase flow*, McGraw-Hill, New York, 1969.
7. D. Gidaspo, *Multiphase Flow and Fluidization – Continuum and Kinetic Theory Descriptions*, Academic Press, San Diego, 1994.
8. D. A. Drew & R. T. Lahey Jr., The Virtual Mass and Lift Force on a Sphere in Rotating and Straining Inviscid Flow, *Int. J. Multiphase Flow*, vol. 13, pp. 113–121, 1987.
9. H. B. Stewart, & B. Wendroff, Two-Phase Flow: Models and Methods, *J. Comput. Phys.*, vol. 56, pp. 363–409, 1984.
10. R. T. Lahey Jr., & D. A. Drew, The Current State-of-the-Art in Modelling of Vapor/Liquid Two-Phase Flows, ASME paper 90-WA/HT-13, 1990.
11. F. H. Harlow & D. Besnard, Well-Posed Two-Phase Flow Equations with Turbulence Transport, *Lett. Math. Phys.*, vol. 10, pp. 161–166, 1985.
12. D. Z. Zhang & A. Prosperetti, Averaged equations for inviscid disperse two-phase flow, *J. Fluid Mech.*, vol. 267, pp. 185–219, 1994.
13. G. E. Fernández, H. E. Ferrari, P. M. Carrica & D. A. Drew, Binary Interaction Force on Spheres II: Inviscid Fluid, *Chem. Eng. Comm.*, vol. 187, pp. 109–128, 2001.
14. G. K. Batchelor & J. T. Green, The hydrodynamic interaction of two small freely-moving spheres in a linear flow field, *J. Fluid Mech.*, vol. 56, pp. 375–400, 1972.
15. G. K. Batchelor, Sedimentation in a dilute dispersion of spheres, *J. Fluid Mech.*, vol. 52, pp. 245–268, 1972.
16. H. Lamb, *Hydrodynamics*, Dover, New York, 1932.
17. L. D. Landau, & E. M. Lifshitz, *Fluid Mechanics*, Pergamon, London, 1959.
18. O. V. Voinov, On the Motion of Two Spheres in a Perfect Fluid, *J. Appl. Math. Mech.*, vol. 33, pp. 638–646, 1969.
19. D. Gidaspo, R. W. Lyczkowski, C. W. Solbrig, E. D. Hughes, & G. A. Mortensen, Characteristics of Unsteady One-Dimensional Two-Phase Flow, *Amer. Nuc. Society Trans.*, vol. 17, pp. 249–250, 1973.
20. J. H. Stuhmiller, The Influence of Interfacial Pressure Forces on the Character of Two-Phase Flow Model Equations, *Int. J. Multiphase Flow*, vol. 3, pp. 551–660, 1977.